www.czasopisma.pan.pl PAN POLSKA AKADEMIA NAUK www.journals.pan.pl

Arch. Metall. Mater. **70** (2025), 4, 1533-1542

DOI: https://doi.org/10.24425/amm.2025.156233

ZIYI TAN[1], SAIHONG TANG[1*], B.T. HANG TUAH BAHARUDIN[1], RONGBIN MA[2*]

ENHANCING HEAVY-DUTY AUTOMOBILE GEAR SURFACES WITH Cr_2O_3-REINFORCED COATINGS: PERFORMANCE ANALYSIS AND SIMULATION

Heavy-duty vehicle gears play a vital role in transmission systems, but the harsh operating conditions they endure often lead to surface wear and deformation. To mitigate these effects, gears must possess optimal hardness and wear resistance. The use of surface coatings has proven to be an effective strategy for enhancing gear performance. In this study, a Cr_2O_3-reinforced coating was applied to gear surfaces using supersonic flame spraying technology. Microstructural, elemental, and phase analyses were carried out using X-ray diffraction (XRD), scanning electron microscopy (SEM), and energy-dispersive spectroscopy (EDS) to evaluate the coating's properties.

The results revealed significant improvements in hardness, adhesion, and wear resistance, with the coated gear exhibiting a more compact surface microstructure. To further assess performance, solid models of both coated and uncoated gears were developed using ANSYS software. Static and fatigue life analyses indicated that the coated gear experienced reduced deformation and a longer service life. This study highlights the effectiveness of Cr_2O_3-reinforced coatings in the durability and overall performance of heavy-duty automotive gears.

Keywords: Heavy-duty vehicle gears; Cr_2O_3 reinforced coating; Performance analysis; simulation

1. Introduction

Gears, a critical component of transmission systems, are gaining increasing importance across a wide range of applications. Among the various factors contributing to gear failures, wear remains a primary cause of premature degradation in service life [1,2]. One effective approach to address this issue is the application of wear-resistant coatings on gear surfaces. Ceramic materials, renowned for their outstanding wear and corrosion resistance, offer a promising solution in this context [3,4]. However, the inherent brittleness and high cost of ceramics have limited their use as bulk components. Instead, ceramic coatings are typically applied to metal substrates such as steel, thereby leveraging the benefits of both material types.

Among these, metal-ceramic coatings have proven especially effective in enhancing the surface properties of the underlying substrate. Notably, Cr_2O_3 coatings have been shown to significantly improve the wear resistance of machine components [5-8]. In addition to their excellent wear performance, Cr_2O_3 coatings also exhibit superior corrosion resistance and chemical stability, ensuring that no harmful substances are released – an attribute that makes them particularly suitable for use in the food industry.

Chromium oxide is an ideal thermal spray material widely used in demanding environments, such as high-temperature and high-emissivity applications, where high-performance requirements must be met under complex conditions. Its suitability arises from several key advantages:

1. It exhibits low sensitivity to overheating during spraying, and even when localized overheating occurs, the coating is unlikely to crack.
2. Chromium oxide spray coatings form an extremely dense layer with strong adhesion to the substrate.
3. This strong bonding and compact structure allow the coating to withstand harsh environmental conditions, making it less susceptible to cracking or delamination.
4. The sprayed layer supports grinding, polishing, and other machining operations, enabling it to meet the precision requirements of various workpiece surfaces.

As shown in Fig. 1, Cr_2O_3 powder has a distinct metallic luster and exists in either a hexagonal or amorphous crystal system. It possesses a high melting point, ranging from 2265 to 2435°C,

[1] UNIVERSITI PUTRA MALAYSIA, FACULTY OF ENGINEERING, SERDANG, SELANGOR, 43400, MALAYSIA
[2] NAHUA NINGBO NEW MATERIALS TECHNOLOGY CO., LTD, NINGBO CITY, 31500, CHINA

* Corresponding author: saihong@upm.edu.my

and a density of 5.2 g/cm^3. Chromium oxide is known for its exceptional hardness and resistance to most acids and bases. These properties, along with excellent corrosion resistance, thermal conductivity, and low friction, make Cr_2O_3 coatings widely applicable across various industrial sectors.

Fig. 1. Cr_2O_3 raw material powder

Surface engineering technologies provide an effective means of significantly enhancing the wear resistance of gears by applying one or more layers of composite wear-resistant coatings to their surfaces. Among such materials, chromium oxide is well known for its excellent sprayability and serves as a highly effective protective coating for metal substrates [9,10]. The resulting Cr_2O_3 coating, characterized by its dark black appearance and dense structure, forms a strong bond with the substrate, facilitating post-treatment processes such as grinding and polishing. However, it is important to note that pure chromium oxide powders tend to have low deposition efficiency, potentially increasing the overall cost of coating production.

To address this challenge, chromium oxide-based wear-resistant coatings can be deposited using techniques such as flame spraying and plasma spraying, both of which are capable of producing relatively dense coatings. For example, Bastakys et al. [11] reported significant improvements in wear resistance by depositing Cr_2O_3 and Cr2O3-SiO_2-TiO_2 coatings on P265GH steel via plasma spraying, achieving a 20-fold reduction in wear rate compared to uncoated substrates. Similarly, Chae et al. [12] used plasma spraying to apply Al_2O_3-40% TiO_2 and Cr_2O_3 coatings on aluminum alloy substrates, with Cr_2O_3 coatings exhibiting lower friction coefficients and superior wear resistance compared to the Al_2O_3-TiO_2 composite.

Extensive investigations into the microstructure, phase composition, and mechanical properties of Al_2O_3, Cr_2O_3, and their composite coatings have consistently shown that single-layer Al_2O_3 and Cr_2O_3 coatings offer excellent adhesion and outstanding wear resistance. Bolelli et al. [13,14] demonstrated that Cr_2O_3 coatings exhibited better wear resistance than Al_2O_3 and Al2O3-13% TiO_2 coatings under friction and wear testing. Additionally, researchers have successfully applied Cr_2O_3 coatings to carbon/carbon (C/C) composite substrates, achieving substantial wear reduction-especially under high loads-thus underscoring their potential to mitigate wear-related material degradation and economic losses [15].

Collectively, these studies affirm that the synergistic interaction between Cr_2O_3 powders and substrates during the spraying process enhances the coating's hardness, corrosion resistance, and wear resistance. This improvement is attributed to the formation of a finer, more uniform microstructure that strengthens interfacial bonding, extends substrate service life, and significantly reduces material loss, energy consumption, and maintenance costs due to wear.

In this context, the present study focuses on Cr_2O_3 as the coating material of choice, owing to its well-established wear and corrosion resistance properties. Using high-velocity oxy-fuel (HVOF) spraying-a form of supersonic flame spraying-Cr_2O_3 coatings were successfully deposited onto 45# steel surfaces [16]. The resulting coatings exhibited low porosity and high bond strength. The primary objective of this study was to investigate the morphology and composition of chromium oxide coatings prepared using HVOF technology, providing valuable insights for the design and optimization of wear-resistant coatings. This research further explores the potential of HVOF-applied Cr_2O_3 coatings to enhance the wear resistance of gears, contributing practical solutions to reduce material degradation and economic loss.

2. Experimental method

2.1. Coating preparation

The coating process was carried out on 45# steel plates using supersonic flame spraying technology. A schematic representation of this method is shown in Fig. 2. The experiment employed a supersonic flame spraying system (HV-8000, Zhengzhou Lijia Thermal Spraying Machinery Co., Ltd.), which included a supersonic flame spray gun and a D-3000 powder feeder. The specific spraying parameters are listed in TABLE 1. The base material used was 45# steel, with sample dimensions of 40 mm × 30 mm × 4 mm. Prior to spraying, the substrate surface was sandblasted, then cleaned ultrasonically with ethanol, and left to stand for two hours. Cr_2O_3 powder was selected as the coating material, with its corresponding properties and parameters detailed in TABLE 3.

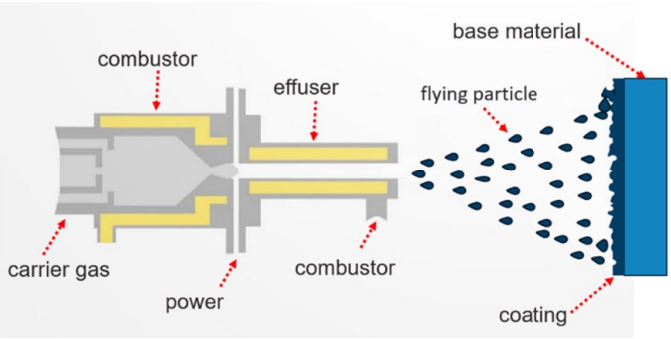

Fig. 2. Schematic diagram of supersonic flame spraying experiment

TABLE 1

Experimental process parameters for spraying

Contents	Parameter
Input power (W)	5000
Fuel pressure (MPa)	1.2
Fuel flow (L/h)	20
Oxygen pressure (MPa)	1.6
Nitrogen Flow Rate (m^3/h)	0.9
Spraying distance (mm)	180
Powder feed rate (g/min)	30

TABLE 2

Material Parameters of 45 # Steel

Carbon content (%)	Density (g/cm^3)	Elastic modulus (GPa)	Poisson's ratio	Tensile strength (MPa)	Yield strength (MPa)
0.42-0.50	7.85	210	0.269	600	355

TABLE 3

Cr_2O_3 Material Parameters

Hardness (HV)	Boiling point (℃)	Melting point (℃)	Specific heat capacity (J/m·K)	Refractivity	Relative molecular mass
2900	3927	2266	0.92	2.5	151.99

2.2. Coating morphology and performance characterization

Following the coating preparation, the samples were trimmed to the required dimensions and polished. The cross-sectional microstructure of the coating was examined using scanning electron microscopy (SEM, ZEISS Gemini300, Zeiss, Germany), while its elemental composition was analyzed via Energy Dispersive X-ray Spectroscopy (EDS). Phase analysis was performed using an X-ray diffractometer, operated at a scanning angle range of 10°-80°, a scan rate of 4°/min, a current of 100 mA, and a voltage of 40 kV. Hardness measurements were conducted using a Vickers hardness tester under a load of 300 g and a dwell time of 10 seconds. A schematic of the hardness testing process is shown in Fig. 3. For each of the four samples, five measurements were taken, yielding average hardness values of 600 HV, 800 HV, 900 HV, and 1070 HV, respectively.

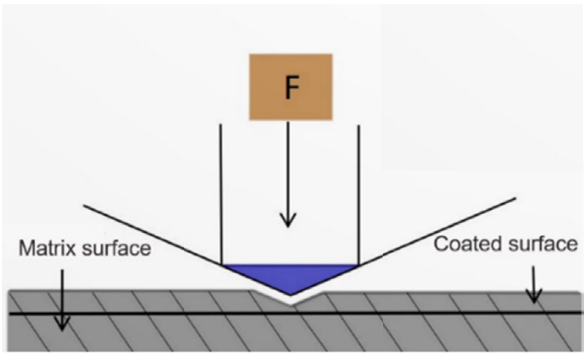

Fig. 3. Schematic diagram of hardness testing

3. Results and discussion

3.1. Surface morphology

In this experiment, four chromium oxide coating samples with varying hardness levels were prepared using the same supersonic flame spraying process. Fig. 4(a) presents a magnified view of the surface morphology of a Cr_2O_3 coating produced by this technique. The surface comprises both fully and partially melted particles, with numerous spherical Cr_2O_3 particles visible, contributing to the coating's high surface roughness. As illustrated in Fig. 4, irregularly shaped pores approximately 30 μm in size are distributed across the surface [17]. These pores tend to cluster, and smaller circular pores are often observed surrounding them [18]. It has been widely reported that coatings with lower porosity, finer grain structures, fewer cracks, and stronger interfacial bonding demonstrate superior wear and corrosion resistance. However, the formation of pores is an inherent characteristic of thermal spraying processes [19,20].

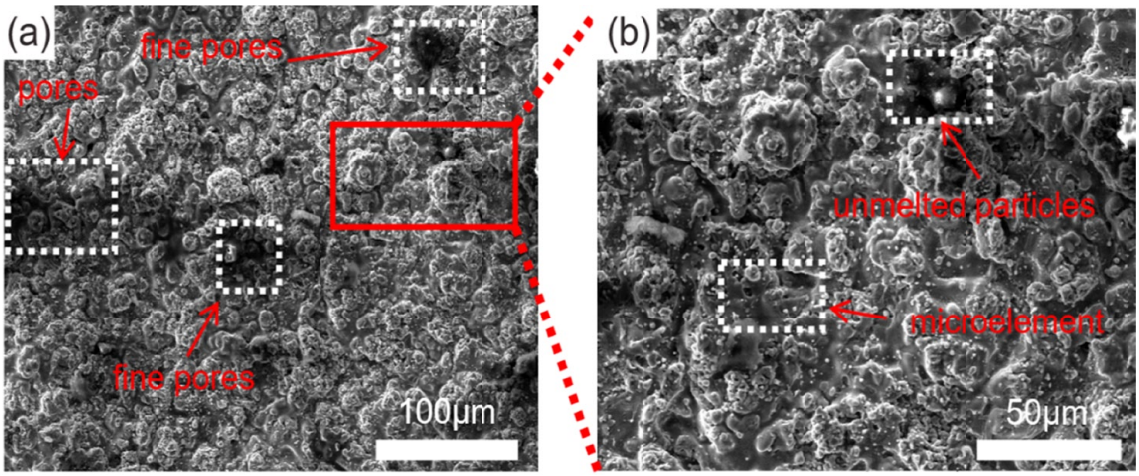

Fig. 4. Surface morphology of the Cr2O3 coating: (a) at 100 μm scale, (b) at 50 μm scale

Several factors contribute to pore formation in thermally sprayed coatings. These include incomplete melting of the feedstock powder, non-uniform pressure distribution from the spray gun, and gas interference during spraying. Additionally, the rapid rise in substrate temperature causes thermal expansion, while subsequent rapid cooling induces residual micro-stresses in the substrate, promoting pore formation. The inherent layered structure of the coating may also facilitate the development of such porosity [21].

As shown in Fig. 4(b), the coating surface contains trace element particles and unmelted particles. Chromium oxide powder includes trace elements that may chemically react with auxiliary gases introduced into the combustion chamber during the high-temperature spraying process. In some instances, the Cr_2O_3 powder does not fully melt, leading to the agglomeration of unmelted particles. This hinders the smooth spreading of molten droplets and results in a convex surface morphology.

3.2. Microscopic morphology of section Cr_2O_3 coating

Fig. 5 presents cross-sectional views of chromium oxide-reinforced coatings with varying hardness levels. In Fig. 5(a), pronounced surface cracks are visible, which may be attributed to prolonged exposure of the coating to air, leading to oxidation and corrosion over time. The corresponding hardness is 600 HV. In practical applications, the bond between the coating and substrate plays a critical role in determining coating performance and service life. Fig. 5(b) shows a cross-sectional view with a hardness of 800 HV. The interface between the substrate and the coating appears well bonded, with no observable voids or cracks, suggesting that the selected supersonic flame spraying parameters are well-suited for preparing Cr_2O_3 coatings.

In Fig. 5(c), the red dashed line highlights surface protrusions and depressions in the coating, likely resulting from the sandblasting treatment conducted prior to spraying. Despite the irregularities, the coating exhibits a hardness of 900 HV. Finally, Fig. 5(d) shows a coating with the highest measured hardness of 1070 HV. The surface roughness imparted by the sandblasting process appears to enhance the mechanical interlocking between the coating and substrate, thereby improving bonding strength.

The coating exhibits an overall layered structure, as illustrated in Fig. 6, which presents a schematic of the spraying process. During spraying, molten droplets are rapidly propelled toward the substrate. Chromium oxide particles, upon multiple

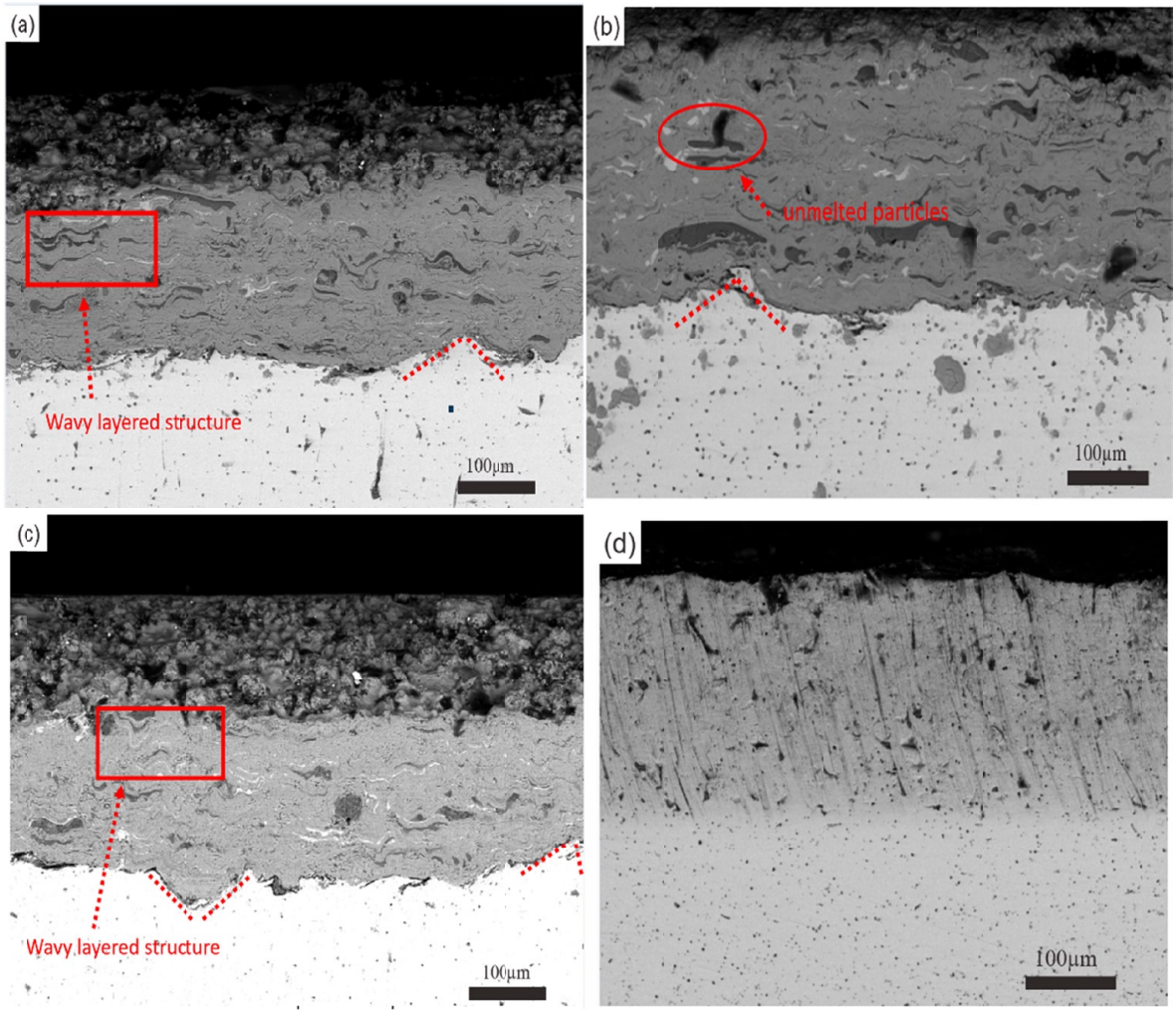

Fig. 5. Microscopic morphology of the cross-section of Cr_2O_3 strengthened coating, (a) 600 Hv, (b) 800 Hv, (c) 900 Hv, (d) 1070 Hv

collisions in their molten state, flatten and accumulate to form a wavy lamellar pattern, often accompanied by interlayer pores. These pores result from incomplete overlap between successive layers and help to relieve thermal stress generated during thermal cycling.

As observed in Fig. 5, unmelted particles are more likely to produce nearly circular structural pores. Incomplete combustion of the powder during spraying may cause unmelted particles to strike the substrate at high velocities, generating recurring thermal residual stresses. These particles can also entrap gases within the coating, leading to the formation of internal pores or microcracks. While such defects may enhance thermal insulation, they also negatively impact the coating's bonding strength, hardness, and wear resistance.

Corrosion can occur at the interface between the coating and the substrate during the spraying process. Although chromium oxide powder possesses strong inherent corrosion resistance, the molten particles, upon exposure to air after ejection from the spray gun, may undergo oxidation. Energy Dispersive X-ray Spectroscopy (EDS) analysis confirms the presence of oxygen (O) elements, and a thin oxide film is observed within the layered structure of the coating. The fine and dispersed Cr_2O_3 powder, in a fully or semi-molten state, is propelled toward the substrate in a confined particle beam. Upon impact, the particles deform due to stamping, forming thin lamellae that adhere to the substrate surface. These lamellae rapidly cool and accumulate, ultimately producing a dense, layered Cr_2O_3 coating. Fig. 6 schematically depicts this deposition process.

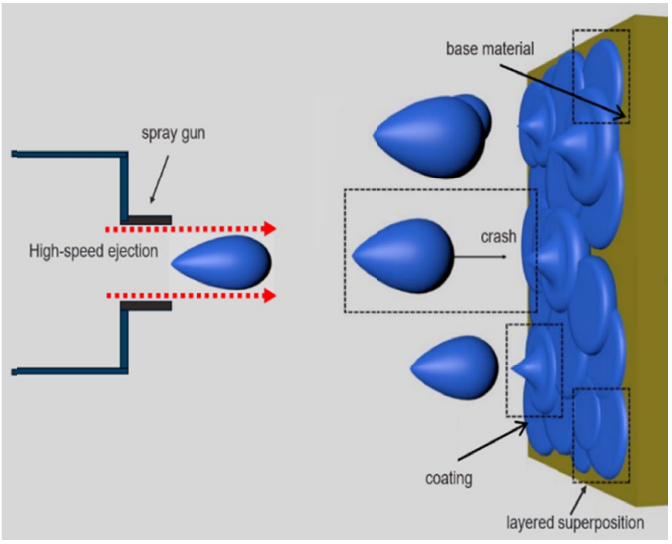

Fig. 6. Schematic diagram of spraying process Cr_2O_3 coating

3.3. EDS analysis of coating

Fig. 7 shows the Energy Dispersive X-ray Spectroscopy (EDS) scan of the prepared Cr_2O_3 coating. The cross-sectional elemental composition includes carbon (C), oxygen (O), silicon (Si), titanium (Ti), chromium (Cr), and iron (Fe). The elemental distribution indicates that trace elements are present in small amounts, primarily concentrated near the upper and lower surfaces of the coating. These trace elements exert minimal influence on the overall performance of the coating. However, the presence of trace elements at the lower interface may slightly affect the coating's bonding strength. Importantly, the high chromium content significantly enhances the mechanical properties of the coating.

To further investigate the oxide composition and the nature of the irregular layered structures, regions within the cross-section exhibiting high oxide concentrations and prominent lamellar features were selected for detailed compositional analysis. The specific area chosen for this analysis is highlighted in Fig. 8.

Fig. 9 presents the elemental distribution map of the selected region, while TABLE 4 summarizes the corresponding elemental composition data. Analysis of the table indicates that chromium (Cr) and oxygen (O) account for approximately 90% of the total composition in the selected area. However, several trace elements are also detected. These trace elements interact with oxygen to form secondary oxides such as MgO, Al_2O_3, and SiO_2.

Magnesium oxide (MgO), known for its high fluidity, can weaken the overall bonding strength of the coating. The forma-

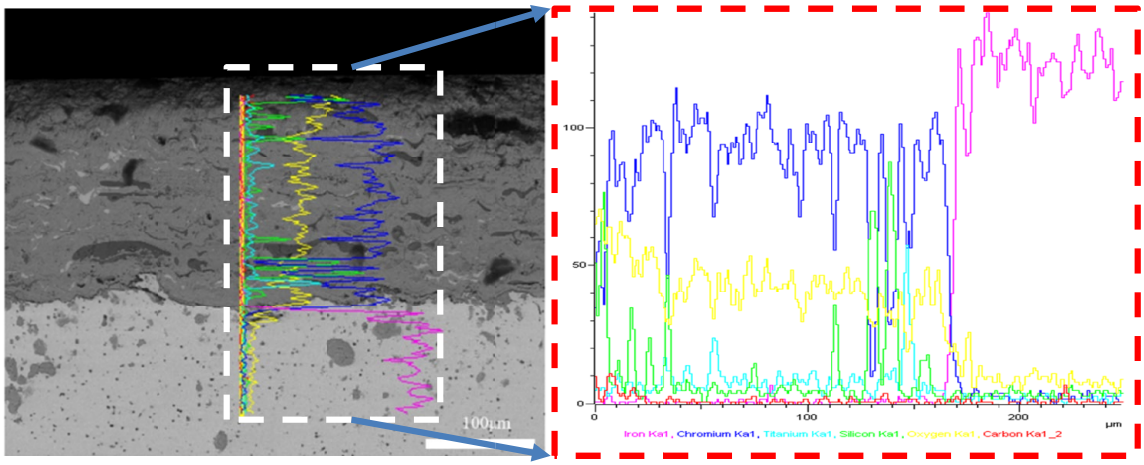

Fig. 7. Energy dispersive spectroscopy (EDS) of Cr_2O_3 coating microstructure

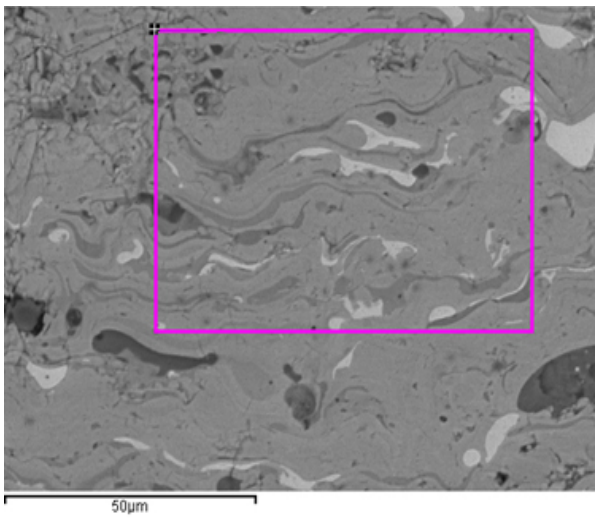

Fig. 8. Energy dispersive spectroscopy (EDS) of Cr_2O_3coating microstructure surface

tion of aluminum oxide (Al_2O_3) requires a significant amount of oxygen and heat, which may hinder the complete melting of the sprayed powder during the deposition process. Silicon dioxide (SiO_2) exhibits behavior similar to that of Al_2O_3, but its presence can also diminish the corrosion resistance of the coating. Furthermore, high concentrations of SiO_2 particles may pose health hazards. Collectively, the presence of these oxides can degrade the coating's mechanical integrity and overall performance.

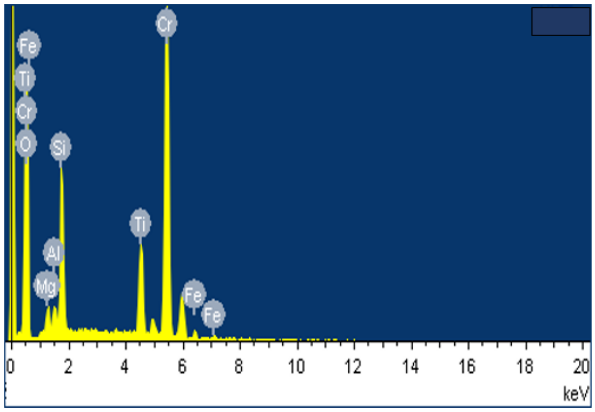

Fig. 9. Cr_2O_3 coating surface scanning element content map

TABLE 4

Specific Element Content

Element	Weight (%)	Atomic ratio (%)
O	30.92	57.69
Mg	0.48	0.60
Al	1.86	2.07
Si	1.39	1.48
Ti	4.68	2.93
Cr	59.68	34.43
Fe	0.99	0.53
Total	100.00	

All of the samples were coated with chromium oxide powder, and the X-ray Diffraction (XRD) patterns for the four hardness samples exhibit a striking similarity, as depicted in Fig. 10. A comparative analysis with the Cr_2O_3 standard card reveals (PDF#38-1479) that the predominant phase in the samples is the Cr_2O_3 phase. Moreover, the phase variations within the same material under different levels of hardness are not substantial. This observation suggests that the Cr_2O_3 material has not undergone significant lattice expansion or contraction.

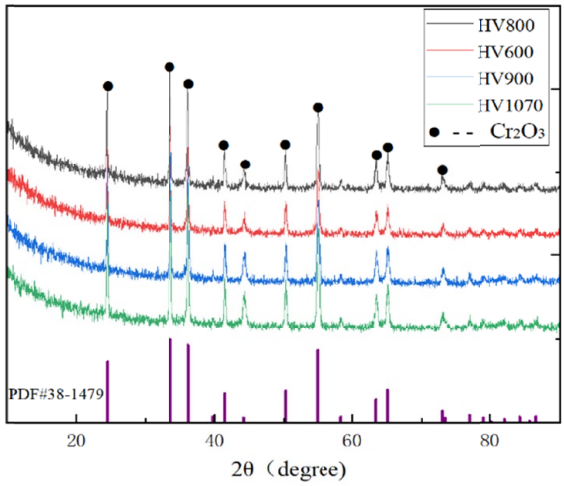

Fig. 10. XRD of Cr_2O_3 coatings with different hardness

3.4. Coating hardness analysis

Five hardness tests were performed on the samples, yielding an average surface microhardness of 800 HV. Fig. 11 includes error bars that provide further insight into data variability. The error bars indicate that the hardness deviations for samples A and C exhibit only minor fluctuations, suggesting that the coating's surface performance is stable. This consistency implies a uniform distribution of the coating powder during the melting process and strong adhesion between the coating and the substrate.

In contrast, sample B shows relatively low hardness within the coating layer, resulting in larger deviations during hardness testing. Although all four samples contain the Cr_2O_3 phase, the observed variation in hardness deviation is greater than expected. A significant difference in average hardness is noted among the samples, with the maximum and minimum values differing by up to 470 HV.

Consequently, a detailed analysis was carried out on the Cr_2O_3 coating with an average hardness of 600 HV. Surface morphology observations revealed that the coating surface was relatively rough and porous, with numerous spherical particles that failed to form a dense structure. Additionally, large pores and cracks were present, likely resulting from solidification shrinkage stress of the molten droplets. Despite these imperfections, the hardness of the Cr_2O_3 coating exceeds that of conventional WC coatings, demonstrating its promising potential for practical applications [22,23].

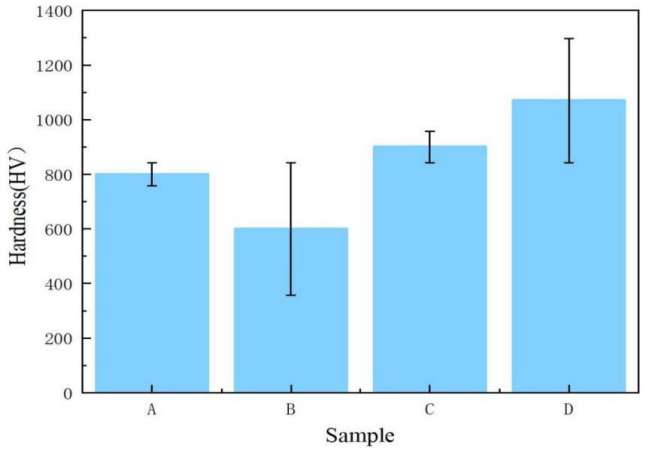

Fig. 11. Coating Microhardness, A – 800 HV; B – 600 HV; C – 900 HV; D – 1070 HV

4. Analysis of coating Model

4.1. Static analysis

A gear model was developed using the three-dimensional simulation software ANSYS. Two configurations, Model A and Model B, were created using structural steel as the base material. Model B incorporated a Cr_2O_3 coating layer, while Model A remained uncoated. The material parameters required for simulation input are detailed in TABLE 5.

Separate simulations were conducted for both the coated and uncoated gear models, evaluating key performance indicators such as total deformation, equivalent elastic strain, and equivalent (von Mises) stress. A comparative analysis of the simulation results was then performed to assess the influence of the Cr_2O_3 coating on the mechanical behavior of the gears, as shown in Fig. 12.

TABLE 5

Testing Material Parameter Settings

Young's modulus (GPa)	Pine to cypress ratio	Density (g/cm³)	Temperature (°C)	Coating thickness (mm)
370	0.22	5.21	18	1

A thorough comparison and analysis of the chart data reveal significant deformation at the gear connection. Examination of the table data shows that the maximum deformation of the gears is substantially reduced after the application of coatings. This

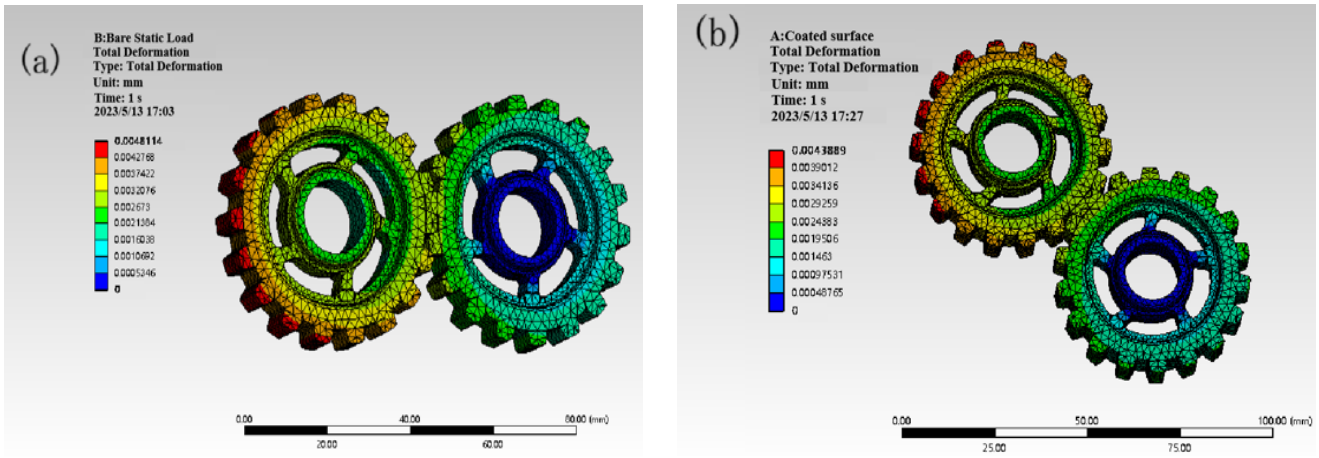

Fig. 12. Total deformation of gears, (a) without coating; (b) Coated

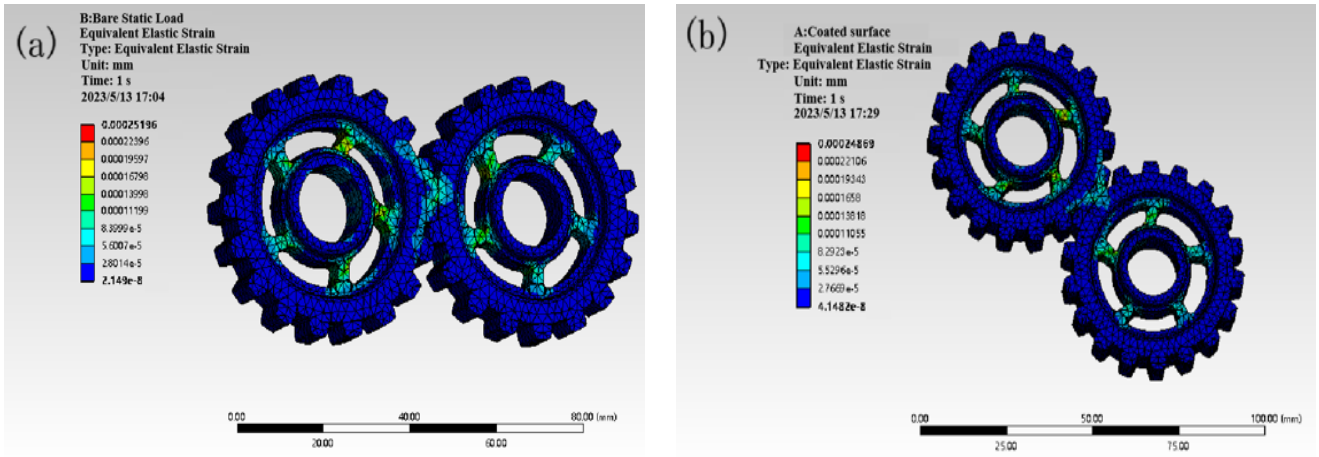

Fig. 13. Equivalent elastic strain of gears, (a) without coating; (b) Coated

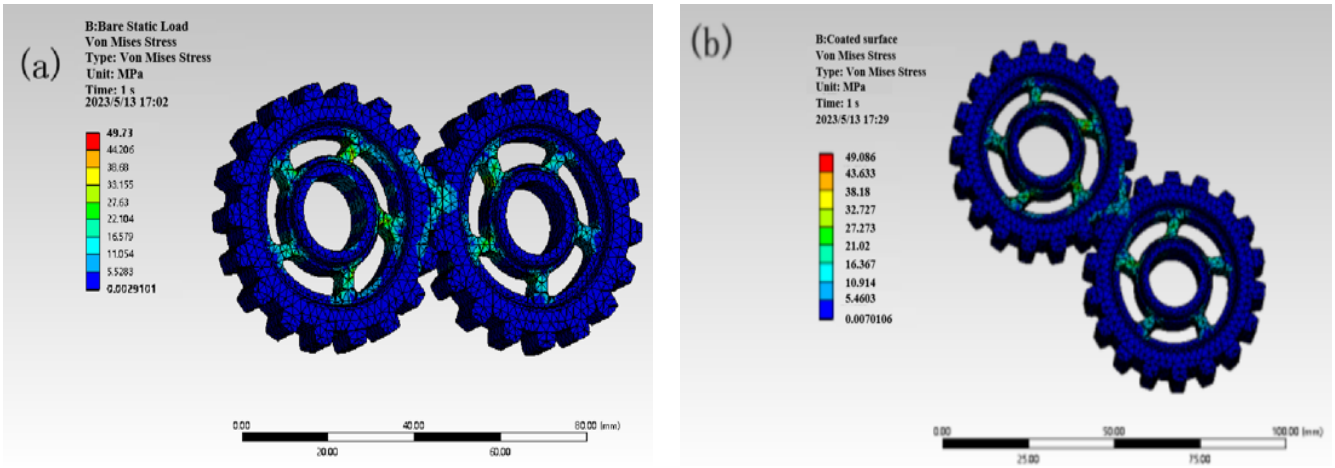

Fig. 14. Equivalent stress of gears, (a) without coating; (b) Coated

suggests that the reinforced coating improves the surface hardness of the substrate, thereby enhancing its load-bearing capacity.

TABLE 6

Static Analysis Data

Content		Uncoated parameters	Coating parameters
Total deformation (mm)	maximum	4.8114e-003	4.3889e-003
	minimum	0	0
Equivalent elastic strain (mm/mm)	maximum	2.5196e-004	2.4869e-004
	minimum	2.149e-008	4.1482e-008
Equivalent stress (MPa)	maximum	49.731	49.086
	minimum	2.9101e-003	7.0106e-003

The equivalent elastic strain in coated gears is reduced, thereby enhancing the overall durability of the workpiece. Additionally, compared to uncoated gears, coated gears exhibit significantly lower equivalent stress. This reduction in equivalent stress indicates improved performance and contributes positively to the fatigue life and strength of the workpiece.

4.2. Fatigue life analysis

A fatigue life analysis is carried out following the static analysis and a comparative assessment of the gear data with and without coatings is performed. The specified lifespan is 270 cycles, with a downward force of 10,000 N applied to the gear contact surface.

When subjecting the gear tooth surface to load, it becomes evident that deformation at the connection beneath the tooth surface is pronounced, resulting in a shorter service life. With the designated service life set at 270 cycles, it is observed that the minimum service life of the gear surface coated with the strengthened coating has increased by 3%, which is 8% higher than that of the uncoated gear. This underscores the substantial enhancement in the gear's intrinsic service life achieved through the application of a strengthened coating.

Simulation analysis further reaffirms that coated gears exhibit an extended service life in comparison to their uncoated counterparts, with a reduced susceptibility to failure. The specific parameters governing this improvement are detailed in TABLE 7.

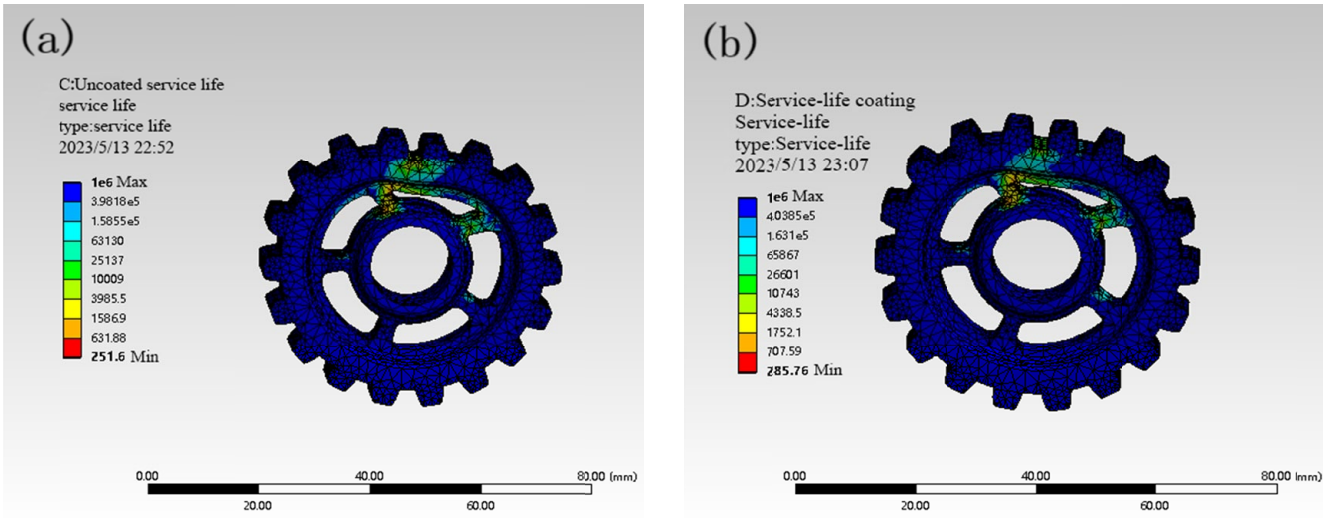

Fig. 15. Gear fatigue life diagram, (a) without coating; (b) Coated

TABLE 7

Fatigue Analysis Data

Content		Uncoated parameters	Coating parameters
Service life (cycle)	maximum	1.6e+002	1.6e+006
	maximum	251.6	285.76
	average	9.1172e+005	9.1718e+005

5. Conclusions

This study utilized supersonic flame spraying technology to apply a Cr_2O_3 coating onto the surface of a 45# steel substrate. Microstructural characterization, elemental distribution, and phase structure analyses were conducted using X-ray diffraction (XRD), scanning electron microscopy (SEM), and energy dispersive spectrometry (EDS). Additionally, surface hardness tests were performed. Finite element modeling and analysis of coated and uncoated gears were carried out using ANSYS software, leading to the following conclusions:

1. The Cr_2O_3 coating produced by supersonic flame spraying exhibits strong surface adhesion, enhanced wear resistance, improved coating performance, and extends the service life of gears.
2. Microstructural analysis indicates a tight bond at the coating-substrate interface. Chromium is the predominant element in the coating composition, reflecting efficient utilization of the coating powder and overall coating stability.
3. Hardness measurements reveal that the presence of an Fe phase in the coating corresponds to relatively high hardness values (approximately 1070 HV). This suggests that incorporating iron powder during the coating preparation can effectively enhance its overall hardness.
4. Comparative simulation analyses between coated and uncoated gears show that coated gears experience significantly reduced surface deformation, which contributes to improved service life.

In future research, the inclusion of various additives to Cr_2O_3 coatings to enhance wear resistance is recommended. Scholars have explored the addition of powders such as Al_2O_3, TiO_2, and TiC to Cr_2O_3, resulting in coatings with superior wear resistance and increased density. Multiple studies have indicated that doped modified chromium oxide composite coatings outperform single-element coatings in various aspects, providing a promising direction for the future development of Cr_2O_3 wear-resistant coatings.

REFERENCES

[1] Xinsheng Wang, Yang Zheng, Jian Liu, Zhihai Cai, Xian Du, Haidou Wang, Study on the enhancement of surface integrity and wear resistance of iron-based coatings by ultrasonic surface rolling process. Journal of Materials Research and Technology **36**, 4898-4912 (2025).

[2] Zhiyuan Wang, Yizheng Chen, Bowen Xu, Yang Liu, Wei Jiang, Fengyuan Bao, Zhiguo Xing, Research on the surface and interface construction behaviour and wear/ corrosion damage mechanism of amorphous high-entropy films based on MAO ceramic phase underlayers. Tribology International **211**, 110829-110849 (2025).

[3] Xinsheng Wang, Zhiguo Xing, Junjian Hou, Wenbin He, Kun Liu, Effect of Adding Ceramic Powder on the Microstructure, Wear and Corrosion Resistance of NiCrBSi/WC coating. Journal of Materials Research and Technology **15**, 4010-4020 (2021).

[4] S.M. Hashemi, N. Parvin, Z. Valefi, Effect of microstructure and mechanical properties on wear behavior of plasma-sprayed Cr2O3-YSZ-SiC coatings. Ceramics International **45** (5), 5284-5296 (2018).

[5] Xinsheng Wang, Jifeng Luo, Yang Li, Honglin Mou, Zhiguo Xing, Zhihai Cai, Shizhong Wei, Yueyang Yu, Properties of laser cladding $(NiCoCr)_{94}Al_3Ti_3$-cBN-hBN hard self-lubricating Ceramic coating. Ceramics International **50** (8), 1371-13769 (2024).

[6] G. Bolelli, D. Steduto, J. Kiilakoski, T. Varis, L. Lusvarghi, P. Vuoristo, Tribological properties of plasma sprayed Cr2O3, Cr2O3-TiO2, Cr2O3-Al2O3 and Cr2O3-ZrO2 coatings. Wear **480**, 1-12 (2021).

[7] M.K. Srinath, J. Nagendra, H.V. Puneeth, M.S. Ganesha Prasad, Micro-structural, physical and tribological properties of HVOF spayed (TiC + Cr2O3) composite coatings. Materials Today: Proceedings **44** (P1), 554-560 (2020).

[8] Xiao Feng, Lin Hongbin, Chen Hui, Du Juan, Miao Jingguo. Effect of Cr2O3 on the Microstructure and Oxidation Resistance of Enamel Coating with TC4 Titanium Alloy. Materials Science **26** (2), 168-172 (2019).

[9] Ehsan Sadri, Fakhreddin Ashrafizadeh, Self-Lubrication Mechanism of Plasma-Sprayed Cr2O3-Ag Nanocomposite Coatings at Room to Moderate Temperatures. Journal of Thermal Spray Technology **30** (6), 1595-1614 (2021).

[10] Sun Huwei, Yi Gewen, Wan Shanhong, Kong Charlie, Zhu Shengyu, Bai Liuyang, Yang Jun, Effect of Cr2O3 addition on mechanical and tribological properties of atmospheric plasma-sprayed NiAl-Bi2O3 composite coatings. Surface & Coatings Technology **427**, 1-14 (2021).

[11] Yanli Wang, Ping Wang, Changxuan Wang, Shenghua Zhang, Preparation and Properties of In Situ Grown Cr2O3 Diffusion Barrier Between Ni Coating and 316L Stainless Steel in Molten Fluoride Salts. Corrosion **77** (7), 753-763 (2021).

[12] Xiong Yang, Jinyan Zeng, Hao Zhang, Jinshuang Wang, Junbin Sun, Shujuan Dong, Jianing Jiang, Longhui Deng, Xin Zhou, Xueqiang Cao, Correlation between microstructure, chemical components and tribological properties of plasma-sprayed Cr2O3 -based coatings. Ceramics International **44** (9), 10154-10168 (2018).

[13] Bastakys Lukas, Marcinauskas Liutauras, Milieška Mindaugas, Grigaliūnas Matas, Matkovič Sebastjan, Aikas Mindaugas, Tribological Properties of Chromia and Chromia Composite Coatings Deposited by Plasma Spraying. Coatings **12** (7), 2-15 (2022).

[14] Young Hun Chae, Seock Sam Kim, Sliding wear behavior of ceramic, plasma sprayed on casting aluminum alloy against SiC ball. Tribology letters **8** (1), 666-670 (2000).

[15] P. Zamani, Z. Valefi, Microstructure, phase composition and mechanical properties of plasma sprayed Al2O3, Cr2O3 and Cr2O3-Al2O3 composite coatings). Surface & Coatings Technology **316**, 138-145 (2017).

[16] Giovanni Bolelli, Valeria Cannillo, Luca Lusvarghi, Tiziano Manfredini, Wear behaviour of thermally sprayed ceramic oxide coatings. Wear **261** (11), 1298-1315 (2006).

[17] Ti Wenhua, Niu Yaran, Li Hong, Zhong Xin, Hong Du, Shi Minhao, Zheng Xuebin, Sun Jinliang, Tribological behavior of plasma-sprayed Cr2O3 coatings on C/C composites sliding against different counterparts. Materials Research Express **8**, 125-136 (2019).

[18] R. Keshavamurthy, J. Madhu Sudhan, Anurag Kumar, Vivek Ranjan, Pratyush Singh, Amandeep Singh, Wear Behaviour of Hard Chrome and Tungsten Carbide-HVOF Coatings. Materials Today: Proceedings **5** (11), 24587-24594 (2018).

[19] Zamani Pejman, Valefi Zia, Jafarzadeh Kourosh, Comprehensive study on corrosion protection properties of Al2O3, Cr2O3 and Al2O3–Cr2O3 ceramic coatings deposited by plasma spraying on carbon steel. Ceramics International **48** (2), 1574-1588 (2022).

[20] Amanov Auezhan, Berkebile Stephen P. Improvement in tribological behavior of thermal spray Cr2O3 and Cr3C2-NiCr coatings by ultrasonic nanocrystal surface modification. Materials Letters **314**, 156-162 (2022).

[21] P. Zamani, Z. Valefi, Microstructure, phase composition and mechanical properties of plasma sprayed Al 2O3, Cr2O3 and Cr2O3 -Al2O3 composite coatings. Surface & Coatings Technology **316**, 1362-1371 (2017).

[22] Pejman Zamani, Zia Valefi, Masoud Mirjani, Effect of grinding and lubricating post-treatment on wear performance of plasma sprayed Cr2O3-Al2O3 composite coatings. Surfaces and Interfaces **16**, 206-214 (2019).

[23] Mao Lin, Xiao Jinkun, Sun Guodong, Wei Xinlong, Wu Duoli, Cao Pan, Zhang Chao, Microstructure and wear behaviors of Cr2O3-Al2O3 composite coatings deposited by atmospheric plasma spraying. Surface & Coatings Technology **444**, 136-144 (2022).